

## Single-Molecule Magnets Constructed from Cyanometalates:



Dongfeng Li,<sup>†</sup> Sean Parkin,<sup>†</sup> Guangbin Wang,<sup>‡</sup> Gordon T. Yee,<sup>\*‡</sup> Andrey V. Prosvirin,<sup>§</sup> and Stephen M. Holmes<sup>\*†</sup>

Department of Chemistry, University of Kentucky, Lexington, Kentucky 40506-0055, Virginia Polytechnic Institute and State University, Blacksburg, Virginia 24061, and Texas A&M University, College Station, Texas 77842-3012

Received November 18, 2004

Treatment of several divalent transition-metal trifluoromethanesulfonates  $[\text{M}^{\text{II}}(\text{OTf})_2]$ ,  $\text{M}^{\text{II}} = \text{Mn}, \text{Co}, \text{Ni}$  with  $[\text{NET}_4][\text{Tp}^*\text{Fe}^{\text{III}}(\text{CN})_3]$  [ $\text{Tp}^* =$  hydridotris(3,5-dimethylpyrazol-1-yl)borate] in DMF affords three isostructural rectangular clusters of  $\{[\text{Tp}^*\text{Fe}^{\text{III}}(\text{CN})_3\text{M}^{\text{II}}(\text{DMF})_4]_2[\text{OTf}]_2\} \cdot 2\text{DMF}$  ( $\text{M}^{\text{II}} = \text{Mn}$ , **3**;  $\text{Co}$ , **4**;  $\text{Ni}$ , **5**) stoichiometry. Magnetic studies of **3–5** indicate that the  $\text{Tp}^*\text{Fe}(\text{CN})_3^-$  centers are highly anisotropic and exhibit antiferromagnetic (**3** and **4**) and ferromagnetic (**5**) exchange to afford  $S = 4, 2$ , and 3 spin ground states, respectively. ac susceptibility measurements suggest that **4** and **5** exhibit incipient single-molecule magnetic behavior below 2 K.

The systematic preparation of cyanometalate networks and clusters has celebrated a resurgence of activity over the past decade.<sup>1</sup> Of these, many species exhibit unusual properties such as room-temperature magnetism,<sup>2</sup> electro-<sup>3</sup> and photo-magnetism,<sup>4</sup> single-molecule magnetism (SMM),<sup>5</sup> charge-transfer-induced spin transitions,<sup>6</sup> compensation behavior,<sup>7</sup> and single-chain magnetism (SCM).<sup>8</sup> Cyanometalates are excellent building blocks for constructing molecule-based clusters and networks because cyanides generally form linear  $\mu$ -CN linkages between two metal centers, stabilize a variety of transition-metal centers and oxidation states, and efficiently communicate spin density information.<sup>1</sup>

Of known cyanometalate clusters, the dominant structural building block contains  $\text{fac-LM}(\text{CN})_3^{n-}$  centers where cyanides link adjacent transition-metal centers and L is a facially

coordinate tripodal ligand.<sup>9,10</sup> Surprisingly, despite the prevalence of poly(pyrazolyl)borates in inorganic chemistry, only tris(pyrazolyl)borate iron(III) tricyanide and a few derived clusters and networks have been described.<sup>5e,8c,10</sup>

As part of a continuing effort to prepare such materials, we have turned our attention toward molecular species that can be systematically substituted via a building block approach, to afford compounds that exhibit tunable magnetic, electrical, and optical properties. Through such a synthetic strategy, we hope to incorporate a series of anisotropic centers to systematically prepare several SMM and SCM materials that

\* To whom correspondence should be addressed. E-mail: smholm2@uky.edu (S.M.H.).

<sup>†</sup> University of Kentucky.

<sup>‡</sup> Virginia Polytechnic Institute and State University.

<sup>§</sup> Texas A&M University.

- (1) (a) Entley, W. R.; Girolami, G. S. *Science* **1995**, *268*, 397–400. (b) Verdager, M.; Bleuzen, A.; Marvaud, V.; Vaissermann, J.; Seuleiman, M.; Desplanches, C.; Scullier, A.; Train, C.; Garde, R.; Gelly, G.; Lomenech, C.; Rosenman, I.; Veillet, P.; Cartier, C.; Villain, F. *Coord. Chem. Rev.* **1999**, *190–192*, 1023–1047. (c) Dunbar, K. R.; Heintz, R. A. *Prog. Inorg. Chem.* **1997**, *45*, 283–291.
- (2) (a) Ferlay, S.; Mallah, T.; Ouahès, R.; Veillet, P.; Verdager, M. *Nature* **1995**, *378*, 701–703. (b) Holmes, S. M.; Girolami, G. S. *J. Am. Chem. Soc.* **1999**, *121*, 5593–5594. (c) Hatlevik, Ø.; Buschmann, W. E.; Zhang, J.; Manson, J. L.; Miller, J. S. *Adv. Mater.* **1999**, *11*, 914–918.

- (3) (a) Sato, O.; Iyoda, T.; Fujishima, A.; Hashimoto, K. *Science* **1996**, *271*, 49–51. (b) Ohkoshi, S.-I.; Sato, O.; Iyoda, T.; Fujishima, A.; Hashimoto, K. *J. Am. Chem. Soc.* **1998**, *120*, 5349–5350.
- (4) (a) Sato, O. *Acc. Chem. Res.* **2003**, *36*, 692–700 and references therein. (b) Arimoto, Y.; Ohkoshi, S.; Zhong, S. J.; Seino, H.; Mizobe, Y.; Hashimoto, K. *J. Am. Chem. Soc.* **2003**, *125*, 9240–9241.
- (5) (a) Sokol, J. J.; Hee, A. G.; Long, J. R. *J. Am. Chem. Soc.* **2002**, *124*, 7656–7657. (b) Choi, H. J.; Sokol, J. J.; Long, J. R. *Inorg. Chem.* **2004**, *43*, 1606–1608. (c) Berlinguette, C. P.; Vaughn, D.; Cañada-Vilalta, C.; Galán-Mascarós, J. R.; Dunbar, K. R. *Angew. Chem., Int. Ed.* **2003**, *42*, 1523–1526. (d) Wang, S.; Zou, J.-L.; Zhou, H.-C.; Choi, H. J.; Ke, Y.; Long, J. R.; You, X.-Z. *Angew. Chem., Int. Ed.* **2004**, *43*, 5940–5943. (e) Schelter, E. J.; Prosvirin, A. V.; Dunbar, K. R. *J. Am. Chem. Soc.* **2004**, *126*, 15004–15005.
- (6) Berlinguette, C. P.; Dragulescu-Andrasi, A.; Sieber, A.; Galán-Mascarós, J. R.; Güdel, H.-U.; Achim, C.; Dunbar, K. R. *J. Am. Chem. Soc.* **2004**, *126*, 6222–6223.
- (7) (a) Ohkoshi, S.; Sato, O.; Iyoda, T.; Fujishima, A.; Hashimoto, K. *Inorg. Chem.* **1997**, *36*, 268–269. (b) Ohkoshi, S.; Abe, Y.; Fujishima, A.; Hashimoto, K. *Phys. Rev. Lett.* **1999**, *82*, 1285–1288.
- (8) (a) Lescouezec, R.; Vaissermann, J.; Ruiz-Pérez, C.; Lloret, F.; Carrasco, R.; Julve, M.; Verdager, M.; Dromzee, Y.; Gatteschi, D.; Wernsdorfer, W. *Angew. Chem., Int. Ed.* **2003**, *42*, 1483–1486. (b) Toma, L. M.; Lescouezec, R.; Lloret, F.; Vaissermann, J.; Verdager, M. *Chem. Commun.* **2003**, 1850–1851. (c) Wang, S.; Zuo, J.-L.; Gao, S.; Song, Y.; Zhou, H.-C.; Zhang, Y.-Z.; You, X.-Z. *J. Am. Chem. Soc.* **2004**, *126*, 8900–8901.
- (9) (a) Yang, J. Y.; Shores, M. P.; Sokol, J. J.; Long, J. R. *Inorg. Chem.* **2003**, *42*, 1403–1419. (b) Shores, M. P.; Sokol, J. J.; Long, J. R. *J. Am. Chem. Soc.* **2002**, *124*, 2279–2292. (c) Sokol, J. J.; Shores, M. P.; Long, J. R. *Angew. Chem., Int. Ed.* **2001**, *40*, 236–239. (d) Heinrich, J. L.; Berseth, P. A.; Long, J. R. *Chem. Commun.* **1998**, 1231–1232. (e) Schelter, E. J.; Prosvirin, A. V.; Reiff, W. M.; Dunbar, K. R. *Angew. Chem., Int. Ed.* **2004**, *43*, 4912–4915. (f) Klausmeyer, K. K.; Wilson, S. R.; Rauchfuss, T. B. *J. Am. Chem. Soc.* **1999**, *121*, 2705–2711. (g) Contakes, S. M.; Kuhlman, M. L.; Ramesh, M.; Wilson, S. R.; Rauchfuss, T. B. *Proc. Natl. Acad. Sci.* **2002**, *99*, 4889–4893.
- (10) (a) Kim, J.; Han, S.; Cho, I.-K.; Choi, K. Y.; Heu, M.; Yoon, S.; Suh, B. J. *Polyhedron* **2004**, *23*, 1333–1339. (b) Lescouezec, R.; Vaissermann, J.; Lloret, F.; Julve, M.; Verdager, M. *Inorg. Chem.* **2002**, *41*, 5943–5945.

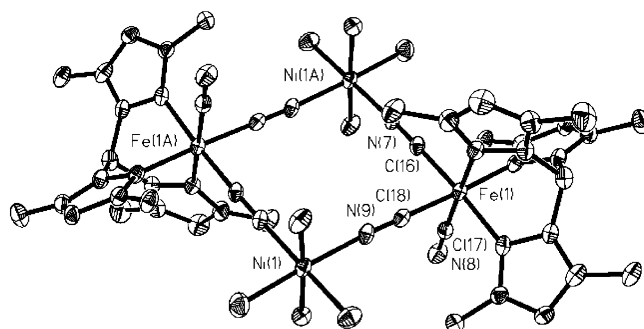
## COMMUNICATION

exhibit high-spin ground states, large and negative axial zero-field splittings, and high blocking temperatures.<sup>5,8–11</sup>

In the present communication, we report the synthetic, magnetic, structural, and spectroscopic details of three isostructural molecular rectangles that are derived from hydridotris(3,5-dimethylpyrazol-1-yl)borate tricyanoferrate(III) and divalent transition-metal centers. Treatment of  $[\text{NEt}_4][\text{Tp}^*\text{Fe}^{\text{III}}(\text{CN})_3] \cdot \text{H}_2\text{O}$  (**1**) or  $[\text{NEt}_4][\text{Tp}^*\text{Fe}^{\text{III}}(\text{CN})_3]$  (**2**) with several divalent transition-metal trifluoromethanesulfonates in DMF readily affords clusters of  $\{[\text{Tp}^*\text{Fe}^{\text{III}}(\text{CN})_3\text{M}^{\text{II}}(\text{DMF})_4]_2\text{[OTf]}_2\} \cdot 2\text{DMF}$  ( $\text{M}^{\text{II}} = \text{Mn}$ , **3**;  $\text{Co}$ , **4**;  $\text{Ni}$ , **5**;  $\text{OTf} = \text{O}_3\text{SCF}_3$ ) stoichiometry in 80–92% yields. The infrared spectra of **3–5** exhibit strong  $\nu_{\text{BH}}$  absorptions at 2543, 2545, and 2547  $\text{cm}^{-1}$ , while the  $\nu_{\text{CN}}$  stretching absorptions are found at 2158, 2150, and 2119  $\text{cm}^{-1}$  for **3**, 2163, 2156, and 2120  $\text{cm}^{-1}$  for **4**, and 2170, 2163, and 2120  $\text{cm}^{-1}$  for **5**. The majority of the cyanide stretching absorptions are shifted to higher energies relative to **1** (2119  $\text{cm}^{-1}$ ) and **2** (2115  $\text{cm}^{-1}$ ), suggesting that bridging cyanides are present in **3–5**. The highest energy  $\nu_{\text{CN}}$  absorptions appear to increase as a function of  $\text{M}^{\text{II}}$  electronegativity, while the lowest energy absorptions are close to those in **2**; these cyanide absorptions are tentatively assigned to bridging and terminal cyanides, respectively.<sup>12</sup>

Compounds **3–5** crystallize in the monoclinic  $P2_1/m$  (**3**) and  $P2_1/n$  (**4** and **5**) space groups.<sup>13</sup> The  $\text{Fe}^{\text{III}}$  and  $\text{M}^{\text{II}}$  centers reside in alternate corners of the rectangular clusters and are linked via cyanides (Figure 1).<sup>10a</sup> A third terminal cyanide per  $\text{Tp}^*\text{Fe}(\text{CN})_3^-$  center remains, and these are related by an inversion center, in an *anti* orientation relative to the  $\text{Fe}_2\text{M}_2$  plane. A single methyl group per  $\text{Tp}^*$  ligand projects perpendicular to and above (ca. 3.65 Å) the  $\text{Fe}_2\text{M}_2$  plane, located opposite the terminal cyanides; the closest contacts between pyrazole rings are ca. 4.42 Å. The  $\text{M}^{\text{II}}-\text{N}$  bond distances are 2.195(4) Å for **3**, 2.083(3) Å for **4**, and 2.041(4) Å for **5**, scaling as a function of increasing  $\text{M}^{\text{II}}$  electronegativity.

In each rectangle, the carbon-bound cyanides give rise to low-spin  $\text{Fe}^{\text{III}}$  ( $S = 1/2$ ), which is expected to exhibit an orbital contribution to the magnetic moment.<sup>5d,9a,11a,14</sup> Consequently, spin-only formulas are not expected to be relevant. If we



**Figure 1.** Partial X-ray structure of **5**. Ellipsoids are at the 50% level, all hydrogen atoms are eliminated, and only DMF oxygen atoms are illustrated for clarity. Selected bond distances (Å) and angles (deg):  $\text{Fe}(1)-\text{C}(16)$  1.928(5),  $\text{Fe}(1)-\text{C}(18)$  1.927(5),  $\text{Ni}(1)-\text{N}(9)$  2.039(4),  $\text{Fe}(1)\cdots\text{Fe}(1A)$  7.461(1), and  $\text{Ni}(1)\cdots\text{Ni}(1A)$  6.972(1) Å;  $\text{C}(16)-\text{Fe}(1)-\text{C}(17)$  86.84(18),  $\text{C}(16)-\text{Fe}(1)-\text{C}(18)$  85.41(18), and  $\text{N}(7A)-\text{M}(1)-\text{N}(9)$  92.34(14)°.

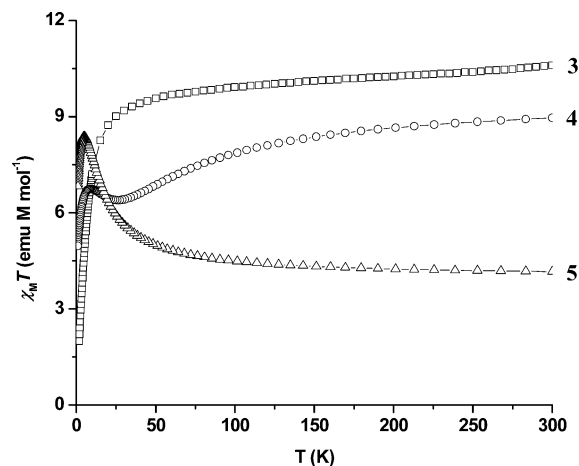


**Figure 2.** Temperature dependence of  $\chi T$  for **3** (□), **4** (○), and **5** (△) in an applied dc field of 1 kG.

assume that the  $\text{Mn}^{\text{II}}$  centers in **3** are high-spin and that  $g_{\text{Mn}}$  is 2, we calculate (from the  $\chi T$  data, crushed crystals) a  $g_{\text{Fe}}$  value of 2.92. Further assuming that this value of  $g_{\text{Fe}}$  does not change for **4** and **5**, we conclude that  $g_{\text{Co}}$  and  $g_{\text{Ni}}$  are 2.84 and 2.38, respectively.

The temperature dependence of  $\chi T$  for **3** suggests that the  $\text{Fe}^{\text{III}}$  and  $\text{Mn}^{\text{II}}$  centers couple antiferromagnetically (Figure 2). Between 300 and 35 K, the  $\chi T$  values gradually decrease from 10.60 to 9.63  $\text{emu K mol}^{-1}$  and then more abruptly below ca. 10 K, reaching a minimum value of 1.99  $\text{emu K mol}^{-1}$  at 1.8 K; similar behavior has been reported for clusters of  $[\text{TpFe}(\text{CN})_3]_2[\text{Mn}(\text{MeOH})_4]$  and  $[\text{TpFe}(\text{CN})_3]_2\text{[Mn}(\text{bpy})_4]_2[\text{ClO}_4]_2$  stoichiometry [ $\text{Tp} = \text{tris}(\text{pyrazol-1-yl})\text{-borate}$ ].<sup>10a</sup> We propose that zero-field splitting of the  $S = 4$  ground state at low temperatures affords lower than expected  $\chi T$  values, rather than intercluster antiferromagnetic interactions, because the closest pyrazole-ring contacts between clusters are ca. 5.434(4) Å.<sup>19</sup>

The temperature dependence of  $\chi T$  for **4** appears to be dominated by spin-orbit coupling effects exhibited by the cobalt(II) centers present (Figure 2). Between 300 and 22 K,  $\chi T$  gradually decreases from 8.90 to 6.55, and this is probably due to depopulation of thermally populated low-lying excited states for the  $S = 3/2$   $\text{Co}^{\text{II}}$  centers. Below 22 K, the  $\chi T$  product increases to a maximum value of 6.65  $\text{emu K mol}^{-1}$  at 10 K and then decreases further to 4.80

- (11) (a) Carlin, R. L. *Magnetochemistry*; Springer-Verlag: New York, 1986. (b) Caneschi, A.; Gatteschi, D.; Lalioti, N.; Sangregorio, C.; Sessoli, R.; Venturi, A.; Vindigni, A.; Rettori, A.; Pini, M. G.; Novak, M. A. *Angew. Chem., Int. Ed.* **2001**, *40*, 1760–1763. (c) Clérac, R.; Miyasaka, H.; Yamashita, M.; Coulon, C. *J. Am. Chem. Soc.* **2002**, *124*, 12837–12844. (d) Gatteschi, D.; Sessoli, R. *Angew. Chem., Int. Ed.* **2003**, *42*, 268–297 and references therein. (e) Kahn, O. *Molecular Magnetism*; VCH Publishers: New York, 1993.
- (12) Nakamoto, K. *Infrared and Raman Spectra of Inorganic and Coordination Compounds*, 5th ed.; Wiley: New York, 1997; Part B, pp 54–58 and 105–116.
- (13) Crystal and structure refinement parameters. **3**:  $\text{C}_{68}\text{H}_{114}\text{B}_2\text{F}_6\text{Fe}_2\text{Mn}_2\text{N}_{28}\text{O}_{16}\text{S}_2$ ,  $P2_1/m$ ,  $Z = 2$ ,  $a = 15.295(3)$  Å,  $b = 13.194(3)$  Å,  $c = 24.321(5)$  Å,  $\beta = 107.09(3)^\circ$ ,  $V = 4691.3(16)$  Å<sup>3</sup>,  $R1 = 0.0655$ ,  $wR2 = 0.1811$ . **4**:  $\text{C}_{68}\text{H}_{114}\text{B}_2\text{F}_6\text{Fe}_2\text{Co}_2\text{N}_{28}\text{O}_{16}\text{S}_2$ ,  $P2_1/n$ ,  $Z = 2$ ,  $a = 15.3587(2)$  Å,  $b = 13.1573(2)$  Å,  $c = 24.1959(4)$  Å,  $b = 108.3940(7)^\circ$ ,  $V = 4639.67(12)$  Å<sup>3</sup>,  $R1 = 0.0492$ ,  $wR2 = 0.0938$ . **5**:  $\text{C}_{68}\text{H}_{114}\text{B}_2\text{F}_6\text{Fe}_2\text{Ni}_2\text{N}_{28}\text{O}_{16}\text{S}_2$ ,  $P2_1/n$ ,  $a = 15.3227(2)$  Å,  $b = 13.13430(10)$  Å,  $c = 24.0570(3)$  Å,  $b = 108.1414(5)^\circ$ ,  $V = 4600.87(9)$  Å<sup>3</sup>,  $R1 = 0.0636$ ,  $wR2 = 0.1740$ . All data were collected on a Nonius Kappa CCD diffractometer at 90.0(2) K using Mo  $K\alpha$  ( $\lambda = 0.71073$  Å) radiation. Structures were solved by direct methods and refined against all data using SHELXL 97.
- (14) Figgis, B. N.; Gerloch, M.; Mason, R. *Proc. R. Soc. London A* **1969**, *309*, 91–118.

emu K mol<sup>-1</sup> at 2 K;<sup>11e</sup> ac susceptibility measurements suggest that intramolecular coupling of Co<sup>II</sup> and Fe<sup>III</sup> centers occurs at low temperatures.

For **5**, the  $\chi T$  product gradually increases between 300 and 165 K. At lower temperatures, the  $\chi T$  rapidly increases to 8.27 emu K mol<sup>-1</sup> at 7 K, suggesting a ferromagnetically coupled  $S = 3$  ground state; below 7 K, the  $\chi T$  product decreases further to 6.71 emu K mol<sup>-1</sup> at 2 K.<sup>18</sup>

Goodenough and Kanamori describe that superexchange between low-spin Fe(III) and the divalent centers should be either antiferromagnetic or ferromagnetic, depending on spin state and orbital symmetry considerations. Assuming, for simplicity, that the Mn<sup>II</sup>( $t_{2g}^3 e_g^2$ ), Co<sup>II</sup>( $t_{2g}^5 e_g^2$ ), and Ni<sup>II</sup>( $t_{2g}^6 e_g^2$ ) centers are octahedral, then the low-spin Fe<sup>III</sup>( $t_{2g}^5$ ) centers should couple antiferromagnetically to Mn<sup>II</sup> and Co<sup>II</sup> (**3** and **4**) and ferromagnetically to Ni<sup>II</sup> (**5**).<sup>11e</sup> However, the clusters are actually of lower symmetry ( $C_2$ ) and the  $t_{2g}$  and  $e_g$  orbitals become nondegenerate, thus complicating simple orbital orthogonality arguments.

Fitting of the magnetic data using the Curie–Weiss equation suggests that antiferromagnetic coupling occurs between cyanide-bridged Fe<sup>III</sup>, Mn<sup>II</sup>, and Co<sup>II</sup> centers while ferromagnetic exchange is present between Fe<sup>III</sup> and Ni<sup>II</sup>. Simulations of the  $\chi T$  versus  $T$  data using MAGPACK<sup>21</sup> allowed for estimations of  $g(M^{II})$  and  $J_{iso}$ ; the calculated values are 2.1 and  $-2.1$  cm<sup>-1</sup> for **3**, 2.7 and  $-10$  cm<sup>-1</sup> for **4**, and 2.2 and 5.3 cm<sup>-1</sup> for **5**.<sup>18</sup> The sign and relative magnitudes of  $\theta$  in **3–5** ( $-8.80$ ,  $-9.61$ , and 4.18 K) are comparable to those of hexacyanoferrate(III) networks of {Mn(OH<sub>2</sub>)<sub>2</sub>[Mn(bpym)(OH<sub>2</sub>)<sub>2</sub>]<sub>2</sub>[Fe(CN)<sub>6</sub>]<sub>2</sub>}<sub>∞</sub> ( $\theta = -12.8$  K),<sup>15</sup> Co<sup>II</sup><sub>3</sub>[Fe<sup>III</sup>(CN)<sub>6</sub>]<sub>2</sub>·6H<sub>2</sub>O ( $\theta = -15$  K),<sup>16</sup> and {[Ni<sup>II</sup>(tn)<sub>2</sub>]<sub>5</sub>[Fe<sup>III</sup>(CN)<sub>6</sub>]<sub>3</sub>]<sub>n</sub>[ClO<sub>4</sub>]<sub>n</sub>·2.5nH<sub>2</sub>O} ( $\theta = 7.45$  K)<sup>17</sup> stoichiometry.

The field dependence of the magnetization for **3–5** suggests that nonlinear magnetization versus applied field effects that grow faster than the Brillouin functions are operative.<sup>11,18</sup> At 1.8 K, the magnetization values for **3–5** are 7.0, 6.6, and 6.11  $\mu_B$ , suggesting spin ground states ( $S$ ) of 4, 2, and 3 for **3–5**, respectively. Assuming  $S = 2$  and 3 ground states for **4** and **5**, fits of the magnetization data using ANISOFIT<sup>20</sup> for  $T \leq 5$  K afford zero-field splitting parameters  $D = -3.04$  and  $-3.98$  cm<sup>-1</sup> and  $g(\text{cluster}) = 3.49$  and 2.44 (Figure 3).<sup>18</sup> Assuming that the sign and magnitude of  $D$  are correct, the spin reversal barrier energies should be  $U = |D|S_1^2 = 12.2$  and 35.8 cm<sup>-1</sup> for **4** and **5**, respectively.<sup>18</sup>

(15) Smith, J. A.; Galán-Mascarós, J.-R.; Clérac, R.; Dunbar, K. R. *Chem. Commun.* **2000**, 1077–1078.

(16) Sato, O.; Einaga, Y.; Fujishima, A.; Hashimoto, K. *J. Am. Chem. Soc.* **1999**, *38*, 4405–4412.

(17) Zhang, S.-W.; Fu, D.-G.; Sun, W.-Y.; Hu, Z.; Yu, K.-B.; Tang, W.-X. *Inorg. Chem.* **2000**, *39*, 1142–1146.

(18) See the Supporting Information.

(19) Chakov, N. E.; Wernsdorfer, W.; Abboud, K. A.; Christou, G. *Inorg. Chem.* **2004**, *43*, 5919–5930.

(20) Shores, M. P.; Sokol, J. J.; Long, J. R. *J. Am. Chem. Soc.* **2002**, *124*, 2279–2292.

(21) (a) Borrás-Almenar, J. J.; Clemente-Juan, J. M.; Coronado, E.; Tsukerblat, B. S. *J. Comput. Chem.* **2001**, *22*, 985–991. (b) Borrás-Almenar, J. J.; Clemente-Juan, J. M.; Coronado, E.; Tsukerblat, B. S. *Inorg. Chem.* **1999**, *38*, 6081–6088.

(22) Rogez, G.; Rebillay, J.-N.; Barra, A.-L.; Sorace, L.; Blondin, G.; Kirchner, N.; Duran, M.; Slageren, J.; Parsons, S.; Ricard, L.; Marvilliers, A.; Mallah, T. *Angew. Chem., Int. Ed.* **2005**, *44*, 1876–1879 and references therein.

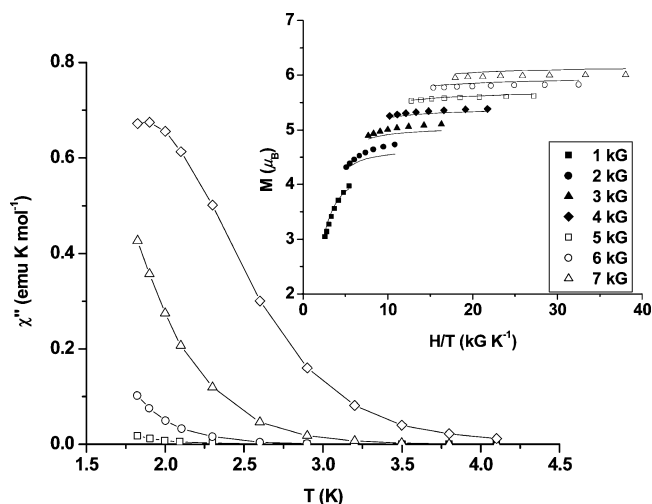


**Figure 3.** Temperature dependence of the imaginary component ( $\chi''$ ) of the ac susceptibility for **5** ( $H_{dc} = 0$  G and  $H_{ac} = 2.5$  G) at 1 ( $\square$ ), 9 ( $\circ$ ), 100 ( $\triangle$ ), and 997 ( $\diamond$ ) Hz. Inset: Plot of reduced magnetization vs  $H/T$  between 1.8 and 5 K. Solid lines represent a least-squares fitting of the data.

ac susceptibility measurements indicate that  $\chi''$  is frequency-independent for **3** and frequency-dependent for **4** and **5**. The frequency dependence of  $\chi''$  for **4** and **5** suggests that the blocking temperatures lie below 1.8 K because frequency-dependent shoulders are readily apparent (Figure 3);<sup>18</sup> such slow magnetic relaxation effects have been previously described for several SMM and SCM derivatives.<sup>5,11d</sup> The frequency dependence of  $\chi''$  exhibits Arrhenius behavior for **5** because plots of  $\ln \tau$  vs  $1/T$  are linear; least-squares fitting indicates that the relaxation time is  $\tau = 7 \times 10^{-7}$  s for **5**. We propose that **5**, and possibly **4**, exhibits incipient single-molecule magnetic behavior below 1.8 K.<sup>18</sup>

In summary, we have described the preparation of three molecular clusters, of which two are likely single-molecule magnets. We anticipate that systematic insertion of paramagnetic transition-metal centers exhibiting greater single ion anisotropy (such as  $4d$  and  $5d$  centers) into this structural archetype will afford additional analogues that exhibit higher spin ground states and blocking temperatures relative to **4** and **5**.<sup>20,22</sup>

**Acknowledgment.** S.M.H. gratefully acknowledges the donors of the American Chemical Society Petroleum Research Fund (PRF 38388-G3), the Kentucky Science and Engineering Foundation (Grant KSEF-621-RDE-006), the University of Kentucky Summer Faculty Research Fellow and Major Research Project programs for financial support. G.T.Y. thanks the National Science Foundation (Grant CHE-0210395) for financial support and A.V.P. (Grant NSF-9974899) is thankful for funds used to purchase the SQUID magnetometer. S.M.H. is also grateful to Eugenio Coronado and Jeffrey R. Long for providing the MAGPACK and ANISOFIT programs.

**Supporting Information Available:** X-ray crystallographic data (CIF format, **3–5**), synthetic details, and additional magnetic data. This material is available free of charge via the Internet at <http://pubs.acs.org>.

IC0483671